

## RESEARCH ARTICLE

# *In Vivo* Magnetic Resonance Imaging of Injected Endothelial Progenitor Cells after Myocardial Infarction in Rats

Yuyu Yao,<sup>1</sup> Yefei Li,<sup>1</sup> Genshan Ma,<sup>1</sup> Naifeng Liu,<sup>1</sup> Shenghong Ju,<sup>2</sup> Jiyang Jin,<sup>2</sup> Zhong Chen,<sup>1</sup> Chengxing Shen,<sup>1</sup> Gaojun Teng<sup>2</sup>

<sup>1</sup>Department of Cardiology, Zhongda Hospital, Southeast University, 87 Dingjiaqiao, Nanjing, Jiangsu, 210009, China

<sup>2</sup>Jiangsu Key Lab of Molecular and Function Imaging, Department of Radiology, Zhongda Hospital, Southeast University, Nanjing, 210009, China

### Abstract

**Purpose:** The purpose of this study was to detect and follow transplanted superparamagnetic iron oxide (SPIO)-labeled endothelial progenitor cells (EPCs) by magnetic resonance imaging (MRI).

**Procedures:** Infarcted rats were randomized to injections of SPIO-labeled EPCs, unlabeled EPCs, or saline. From 1 day to 8 weeks, *in vivo* serial MRI was performed for cell tracking.

**Results:** Labeled cells were visualized as hypointense areas by MRI. The presence of labeled EPCs at 10 days and disappearance of these cells by 8 weeks was confirmed by iron and 4',6-diamidino-2-phenylindole. Co-staining for iron and ED-1 showed that the iron-positive cells were macrophages. EPC implantation significantly elevated vascular endothelial growth factor expression, accompanied by increased capillary and arteriole density in the ischemic myocardium.

**Conclusions:** At 8 weeks, the transplanted EPCs were not present and the enhanced MRI signals arose from macrophages. However, both EPCs enhanced cardiac function. The major mechanism of cardiac improvement appears to be paracrine pathways of the engrafted EPCs.

**Key words:** *In vivo* tracking, Magnetic resonance imaging, Endothelial progenitor cells, SPIO, Myocardial infarction

## Introduction

I schemic heart disease is the leading cause of morbidity and mortality in industrialized countries [1]. Implantation of bone marrow-derived stem cells shows therapeutic potential for the repair of myocardial infarction (MI) [2]. However, results from randomized clinical trials of stem cell therapy for MI have yielded mixed results, with some studies reporting significant improvement in cardiac function [3] and others showing no effects [4]. The observed failure of engraftment could be due to delivery techniques, the number of engrafted cells, and/or other unknown causes. It is

critically important to understand the underlying stem cell biology which requires the use of molecular markers to determine the nature and track the long-term fate of the transplanted cells [5]. Studies have demonstrated that very few stem cells localize within a specific target area, making it difficult to assess the exact fate of implanted cells [6]. Therefore, the development of imaging strategies that can monitor graft survival, track cell migration, and integration is crucial.

Magnetic resonance imaging (MRI) is the imaging modality used by most research studies to noninvasively evaluate stem cells *in vivo*. MRI has excellent soft tissue contrast, high anatomical detail, and minimal invasiveness. MRI has the ability to monitor stem cell homing or provide dynamic assessment of cell migration into the targets [7].

Cells labeled with iron oxide or other paramagnetic probes lead to reduced T2 and signal intensity of the surrounding protons [8]. Superparamagnetic iron oxide (SPIO)-laden cells have been detected after injection into the infarcted myocardium of mouse, rabbit, and pig [9–11]. Adult bone marrow is a rich reservoir of tissue-specific stem and progenitor cells. A scarce population of bone marrow cells known as endothelial progenitor cells (BMEPCs) has a potential angiogenic effect and contributes to the revascularization of ischemic areas [12]. However, cells in the transplanted tissue were identified only in postmortem histology, making the fate and movement of transplanted cells uncertain.

In the present study, we focused on two objectives: (1) to examine whether intramyocardial transplantation of rat BMEPCs could survive, enhance neovascularization, and improve left ventricular function after chronic MI and (2) to test the function of SPIO-labeled vs. unlabeled cells, as well as serial imaging of labeled BMEPC migration to the ischemic area.

## Methods

### *Rat EPC Preparation*

Endothelial progenitor cells (EPCs) were isolated from the tibias and femurs of 4-week-old male Sprague–Dawley (SD) rats (Shanghai Laboratory Animal Center of the Chinese Academy of Science). Aspirated bone marrow was mixed with 1,000 U/mL heparin in phosphate-buffered saline (PBS). The mononuclear cell fraction was obtained from a Lymphoprep density gradient (Sigma, St. Louis, MO) after centrifugation. The mononuclear cell fraction was collected, washed, and centrifuged. The cell pellet was suspended in growth factor-supplemented EBM-2 medium (Lonza, Walkersville, MD) and plated on fibronectin (FN; Sigma)-coated flasks. After 48 h, the non-adherent cell population was transferred to a new FN-coated plate to remove rapidly adherent hematopoietic cells; only the non-adherent cell population was harvested for further evaluation in all experiments. Spindle-shaped cells were observed after 4 days.

Cells were primarily characterized by phase contrast microscopy evaluating cobblestone morphology. Cells were incubated with acLDL-Dil for 4 h at 37°C. Lectin binding was analyzed using fluorescein isothiocyanate (FITC)-conjugated UEA-1-lectin (Sigma). Cells were then examined under a fluorescence microscope. Immunocytochemistry was used to analyze the expression of various progenitor and endothelial lineage markers such as KDR/Flk-1, eNOS, CD31 (Santa Cruz Biotechnology, Santa Cruz, CA), and CD34 (Dako, Glostrup, Denmark).

The EPCs were used between culture passages 3 and 6. The cultured EPCs were incubated with the labeling medium containing 25 µg/mL SPIO (Resovist, Schering AG, Berlin) and 0.375 µg/mL poly-L-lysine for 18 h in a 25-cm<sup>2</sup> flask. Prussian blue staining was performed, and labeling efficiency was determined by manual counting of stained and unstained cells at ×100 magnification. Labeling efficacy was also checked with T2-weighted MRI. Different concentrations of labeled cells were suspended in agarose to determine the ability to track cells.

The effect of SPIO labeling on cell viability and proliferation was tested using the methyl thiazolyl tetrazolium (MTT) assay. SPIO-labeled and unlabeled EPCs were grown in a 96-well plate. After 4 days, MTT was added. The 570-nm wavelength of light absorption was employed for measurement of the light absorption value of every well in a spectrophotometer (Bio-Rad Laboratories, Hercules, CA).

To evaluate the incorporation of EPCs into the ischemic myocardium, SPIO-labeled and unlabeled cells were also labeled with the fluorescent dye 4',6-diamidino-2-phenylindole (DAPI, Sigma). For fluorescent labeling, DAPI was added to the culture medium at a final concentration of 50 µg/mL. After 2 h of incubation, labeled cells were washed with PBS three times to remove the excess DAPI, trypsinized, and collected for the subsequent studies.

### *Rat Model of Myocardial Ischemia and EPC Transfer*

SD rats weighing 250±30 g were purchased from the Shanghai Laboratory Animal Center of the Chinese Academy of Science. They were housed with a 12/12-h dark/light cycle with water and standard chow diet ad libitum. The study complied with standards for the care and use of laboratory animals (Laboratory Animal Center of Southeast University). Rats were subjected to ligation of the left coronary artery. Briefly, a thoracotomy was performed via the fourth intercostal space, the heart was exposed, and ECG was then monitored. A 6–0 polypropylene suture was passed loosely around the left anterior descending (LAD) coronary artery near its origin. Once hemodynamics was stabilized, LAD occlusion was performed by tightening the suture loop. Acute myocardial ischemia was deemed successful on the basis of elevation of the ST segment on ECG.

Ninety rats were included in the study and were divided into the MI group ( $n=80$ ) or sham MI group ( $n=10$ ). Among the rats with MI, 20 died within 4 h after the surgical procedure. Sixty rats with MI were included in functional and morphometric evaluation by echo and MRI. MI rats were randomly divided into three groups: those receiving  $1 \times 10^6$  SPIO-labeled EPCs, those receiving  $1 \times 10^6$  unlabeled EPCs, and those receiving PBS by direct injection into the infarct area. All rats underwent serial MRI examinations for cell tracking at 24 h, 10 days, 4 weeks, and 8 weeks after MI and were euthanized at 24 h ( $n=12$ ), 10 days ( $n=24$ ), and 8 weeks ( $n=24$ ) after MI to confirm MRI results. 2,3,5-Triphenyltetrazolium chloride (TTC) staining was performed 24 h after MI, and echo and histological analysis were performed 10 days after MI.

Cyclosporin A (50 mg/kg, HuaBei Pharmacy, Shijiazhuang) was administered orally in all groups by daily oral gavage starting on the day of transplantation for immunosuppressive treatment.

### *EPC Tracking by MRI*

Cardiac MRI was performed at 24 h, 10 days, 4 weeks, and 8 weeks post-MI using a 7T Bruker PharmaScan and Paravision software (PV5.0, Bruker, Germany). Rats were anesthetized with 1.0% isoflurane (KeYuan, ShanDong) in 1 L/min of oxygen and monitored using a small animal instrument monitoring and gating system for respiration rate and cardiac triggering. Images were obtained with a conventional cardiac-gated fast low-angle shot (FLASH) sequence. The field of view was 6×6 cm and a 256×256 matrix was employed, yielding an in-plane resolution of 234×234 µm. The images were acquired from successive slices along the

short cardiac axis (short axis) with a slice thickness of 1 mm; 16 frames were prescribed from apex to base. The repetition time was 70 ms, echo time was 2.5 ms, and flip angle was 60°. The entire imaging protocol was performed in the range of 15 min.

Gadodiamide is a commonly used MRI contrast agent that results in delayed contrast enhancement of an injured myocardium and areas at risk for infarct. Gadodiamide (0.2 mmol/kg, Bayer Schering Pharma) was injected via the tail vein 10 min before imaging at 24 h after MI. The MRIs were analyzed using ImageJ 1.41 software (NIH). Infarct sizes were determined manually by analysis of Gd-DTPA-enhanced regions. Slice hyperintense areas were then summed to generate infarct volume as a percentage of left ventricle (LV) myocardial volume.

### *Histological Analysis*

After the MRI acquisition at 24 h, 10 days, and 8 weeks post-MI, rats were euthanized with sodium pentobarbital (50 mg/kg, IP).

To measure infarct size at 24 h after MI, the heart was cut into five transverse slices from apex to base, each approximately 2 mm thick. Slices were incubated with 2% TTC (Sigma) for 5 min at 32°C in which the viable myocardium stained red and the infarcted area stained white. Each slice was digitalized using a scanner. ImageJ was used for manual planimetry of the LV border and infarct region on TTC images. Infarct volume was calculated as a percentage of total LV volume and was compared with MRI results in a blinded manner.

In the 10-day and 8-week groups, the heart was rapidly excised after PBS perfusion. Cardiac tissues were fixed with 4% paraformaldehyde and embedded. Four-micrometer sections were obtained for morphological analyses. Sections were subjected to Masson's trichrome staining or immunohistochemical analysis using a staining kit (Vector Laboratories, Burlingame, CA) according to the manufacturer's instructions. Primary antibody against ED-1 (Chemicon, Temecula, CA, 1:200) was used for immunostaining of monocytes/macrophages. The number of ED-1-positive cells was counted in a double-blind fashion from ten different fields of each section ( $n=6$ ) at  $\times 400$  magnification. Prussian blue staining was performed to detect SPIO-labeled cells. Double staining was performed for ED-1 and Prussian blue staining. For immunostaining, the following primary antibodies were used: CD31,  $\alpha$ -smooth muscle actin (SMA), and vascular endothelial growth factor (VEGF) (Santa Cruz Biotechnology, 1:200). Angiogenesis was quantitatively assessed by CD31-positive staining for the determination of capillary density and  $\alpha$ -SMA-positive staining for the determination of arteriolar density. Capillaries were identified as having a diameter  $<20$   $\mu\text{m}$  and a layer of endothelial cells without smooth muscle cells, whereas arterioles were identified as having a diameter  $>20$  and  $<100$   $\mu\text{m}$  with a layer of smooth muscle cells. To determine capillary density and artery density, the number of positive staining was counted in a double-blind fashion from ten different fields of each section in the peri-infarct zone ( $n=8$ ). The average number of the vessels in one section was used for the assessment of vascular density.

### *Functional Assessment*

A Vevo 770 echocardiography system (VisualSonics, Toronto, ON, Canada) with a 12-MHz transducer was used. Under mild isoflurane anesthesia, echocardiography was performed in the 10-day and 8-week post-MI groups.

In the 8-week group, hemodynamic parameters were measured by carotid cannulation using a 2.5-French micro-manometer (Millar Instrument) by advancement into the left ventricle. Mean arterial pressure, cardiac contractility ( $dP/dt$  maximum,  $dP/dt$  minimum), and left ventricle end diastolic pressure (LVEDP) were analyzed using Chart for Windows (version 4; AD Instruments).

### *Quantitative Real-Time PCR*

Total RNA was extracted from infarct myocardium using Trizol reagent (Invitrogen, Carlsbad, CA) in the 10-day groups. cDNA was transcribed using a cDNA Archive Kit (Applied Biosystems, Foster City, CA). Quantitative real-time PCR was carried out using the Gene Expression Assay Rn00582935\_ml for VEGF running on a 7500 real-time PCR system (Applied Biosystems). Transcription of the housekeeping gene GAPDH was determined by specific primer/probe mix. The final quantification was determined by Relative Quantification software (Applied Biosystems).

### *Statistical Analysis*

Data were compared among experimental groups using ANOVA followed by Fisher's PLSD. Data were expressed as mean  $\pm$  SEM. Differences were considered statistically significant at a value of  $P<0.05$ . A Pearson correlation coefficient analysis was calculated to describe the relationship between EPC numbers in infarct area with left ventricular contractility.

## **Results**

### *Characteristics of EPCs*

Bone marrow mononuclear cells were separated by density gradient centrifugation and differentiated into "late EPCs" after a longer culture period (three to six passages). Late EPCs exhibited cobblestone-like morphology typical of endothelial cells (Fig. 1a). Additionally, endothelial cell phenotype was characterized by assessing acLDL-Dil uptake and FITC-conjugated UEA-1-lectin binding (Fig. 1a). Furthermore, EPCs were positive for a panel of endothelial cell markers, including CD31, KDR, CD34, and eNOS (Fig. 1b). The cells were therefore confirmed as BMEPCs. A labeling efficiency of 100% was observed for SPIO in EPCs. SPIO-labeled EPCs showed abundant intracytoplasmic blue inclusions by Prussian blue staining. The magnetic properties of labeled cells were assured by MRI scans of agar phantoms prepared from cell suspensions. A good correlation between the number of labeled cells and T2 relaxometry in the MR images was observed. A phantom of  $1 \times 10^6$  cells appeared black, whereas a phantom of  $0.1 \times 10^6$  cells appeared gray (Fig. 1d).

The absorbencies of the SPIO-labeled and unlabeled EPCs were  $0.56 \pm 0.01$  and  $0.53 \pm 0.01$ , respectively. There were no significant differences in cell viability between the two groups by MTT assay ( $P>0.05$ ,  $n=8$ ), indicating that the labeling method poses little effect on cell viability.

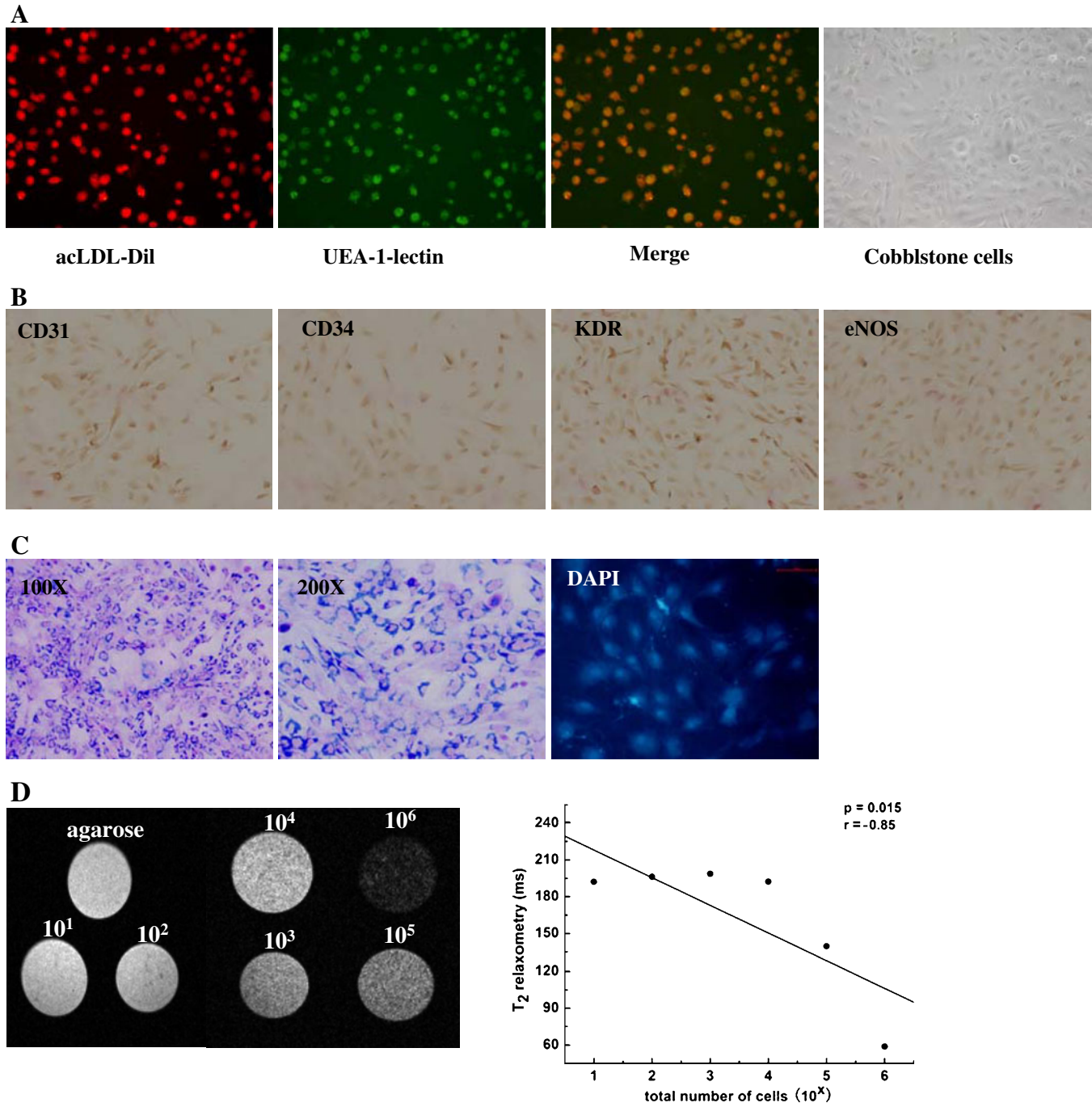


**Fig. 1.** Characterization of cultured BMEPCs. **a** At day 7 after the isolation, adherent cells intensively took up acLDL and bound an endothelial-specific lectin as revealed by fluorescence microscopy. **b** Positive for CD31, VEGFR2 (KDR), CD31, and eNOS. **c** Prussian blue-stained SPIO-labeled EPCs (25  $\mu\text{g}/\text{mL}$ ). DAPI-labeled EPCs ( $\times 200$  magnification). **d** Sensitivity of *in vitro* MRI of SPIO-labeled EPCs. Cell numbers ranging from  $1 \times 10^1$  to  $1 \times 10^6$  were scanned after treatment with SPIO for 18 h. *In vitro* cells MRI, T2-WI of seven Eppendorf tubes, images of SPIO-labeled EPCs showed increased hypointensity as the number of cells was increased (from  $10^1$  to  $10^6$ ).

### MRI-Guided EPC Tracking in Rats with and without MI

In the MI 1-day groups, gadodiamide was administered as a contrast enhancement agent to aid in the identification and quantification of the infarcted region, which appeared white

in these images; the borders between hyperintense areas and non-enhanced areas were distinct (Fig. 2a). MR images and corresponding TTC slices obtained in a rat after gadodiamide injection are depicted in Fig. 2b. Delayed hyper-enhancement was clearly visualized in the anterior left ventricular walls corresponding to the infarcted myocardium

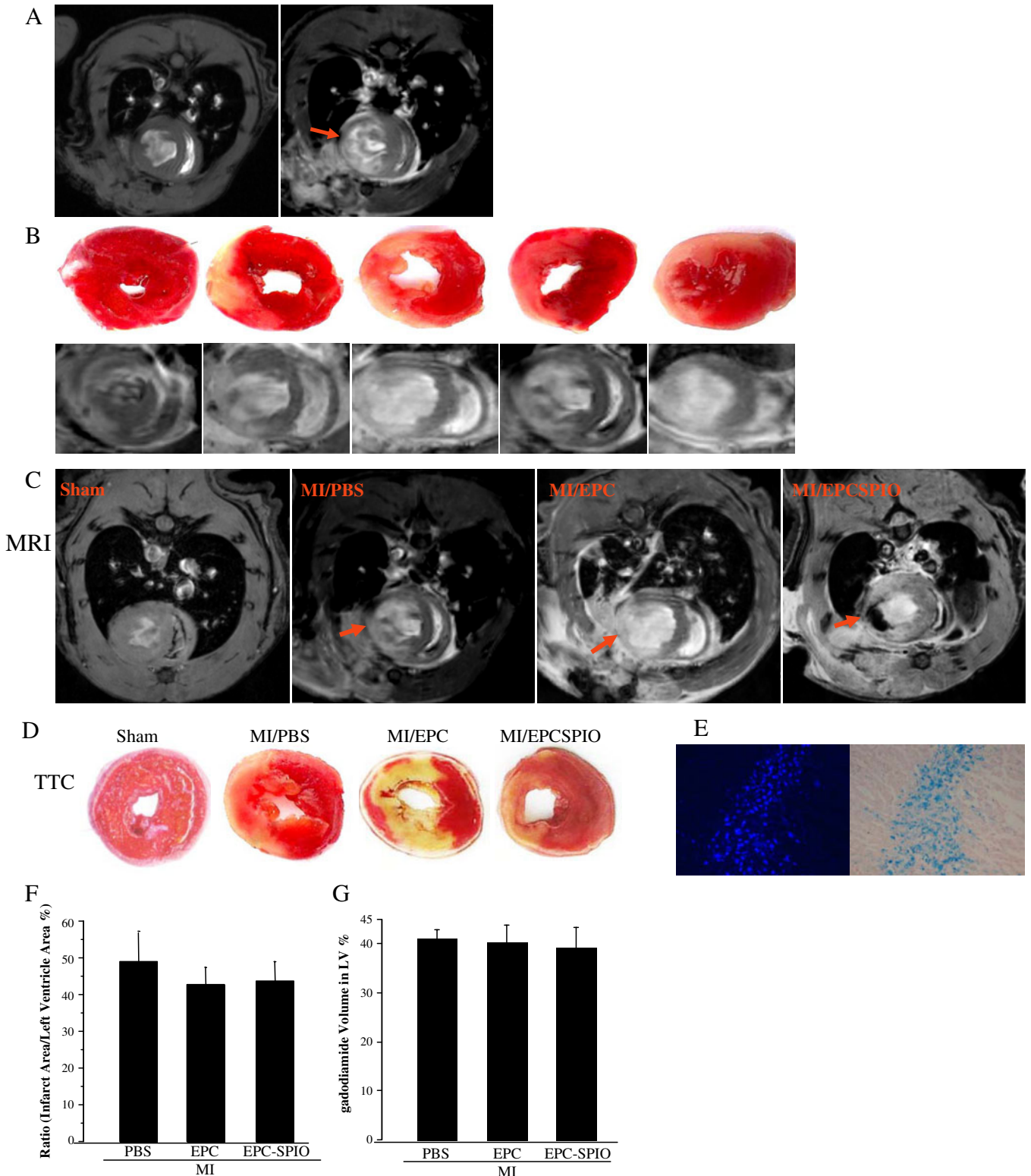


**Fig. 2.** Representative short-axis delayed contrast-enhanced (DCE) image in rats acquired at 7T using FLASH sequence. **a** Twenty-four hours after MI, gadodiamide results in delayed contrast enhancement of injured portions of the myocardium and areas at risk for infarct of the same rat were compared. MRI can differentiate viable and non-viable (red arrow) myocardial tissue. **b** Example of MR images and corresponding TTC slices obtained in a rat after gadodiamide injection. **c** The bright hyper-enhanced region (arrows) corresponds to infarcted myocardium 10 min post-gadodiamide injection. **d** Representative postmortem TTC staining ( $\times 10$  magnification). **e** Histologic section with Prussian blue stain 1 day after SPIO-labeled EPC injection ( $\times 200$  magnification). **f** Quantitative analysis of infarct volume (TTC). **g** Percentage of DCE myocardial volume at 24 h after MI.

in the MR images of heart slices from all three MI groups (Fig. 2c). In addition, round hypointensities were observed at the region of cell injection in all rats injected with SPIO-labeled EPCs. TTC staining directly corresponded to MRI results (Fig. 2d). No apparent difference in myocardial infarct size was observed in all three MI groups 1 day after MI (Fig. 2f, g).

We performed serial MRI exams to track the cells at 10 days, 4 weeks, and 8 weeks after cell injection into the infarct area of the LV. Areas with hypointensity were still visualized in rats receiving SPIO-labeled EPCs and were attenuated at 8 weeks after MI. There were no hypointense lesions in myocardial regions in MI control and MI/EPC (unlabeled) hearts. We also observed the progression of ventricular remodeling that developed as a consequence of MI from 10 days to 8 weeks, including thinning of the anterior wall of the left ventricle and expansion of the left ventricular chamber (Fig. 3a, e).

### *EPCs Improved Cardiac Function After MI*

We used two methods to evaluate cardiac function after EPC transplantation in MI model. At 10 days and 8 weeks after MI, transthoracic echocardiographic examination was performed. MI caused a significant increase in systolic (LVIDs) and diastolic left ventricular inner diameter (LVIDd), whereas LV ejection fraction and fractional shortening (FS) were significantly reduced (Table 1). Both SPIO-labeled and unlabeled EPCs attenuated LV dilatation and dysfunction compared to the MI control group. We observed a positive correlation between the number of EPCs in infarct area and LVEF (Pearson correlation coefficient;  $r=0.741$ ,  $P=0.002$ ).

The effects of EPC transplantation on hemodynamic parameters 8 weeks after MI are shown in Table 2. MI induced a fivefold increase of LVEDP compared to the sham group, whereas EPC transplantation significantly reduced LVEDP. Cardiac contractility was markedly reduced after MI, but was significantly increased by EPC transplantation. No significant difference between labeled and unlabeled cells was observed at 8 weeks.

### *EPC Transfer Reduced Apoptosis and Inflammatory Cell Accumulation*

Apoptotic cardiomyocytes were detected by TUNEL staining in the peri-infarcted region 10 days after MI (Fig. 4a). The ratio of TUNEL-positive cardiomyocytes to total number of cardiomyocytes in both EPC transplantation groups was significantly reduced compared to the MI control group (Fig. 4b).

Inflammatory cell accumulation in the infarcted region of the heart was identified by ED-1 immunostaining 10 days after MI (Fig. 4c). ED-1-positive cells were counted for the quantification of monocyte/macrophage number (Fig. 4d). Increased inflammatory cell infiltration was detected in the infarct area of the heart after MI; however, transplantation of

**Fig. 3.** Serial *in vivo* tracking of EPCs by MRI. **a** *In vivo* MRI 10 days after EPC injection and sham operation. **b** Histologic section with Prussian blue stain 10 days after SPIO-labeled EPCs injection ( $\times 200$  magnification). **c** Representative Masson's trichrome staining ( $\times 10$  magnification) and quantitative analysis of infarct size. **d** Representative Prussian blue and DAPI co-staining in the SPIO-labeled EPC injection group. Several cells showed Prussian blue and ED-1 co-staining 10 days after MI. **e** Short-axis FLASH sequence of rat with SPIO-labeled EPCs injection shows the distinct signal dropout (arrow) that is not observed in the control rat (4 and 8 weeks). **f** Representative Masson's trichrome staining in the 8-week group ( $\times 10$  magnification). **g** Representative Prussian blue and ED-1 double staining in SPIO-labeled EPC injection group 8 weeks after MI.

unlabeled and labeled EPCs significantly decreased the number of ED-1-positive cells compared with the MI control group.

### *EPC Transfer Increased Neovascularization in the Border Zone*

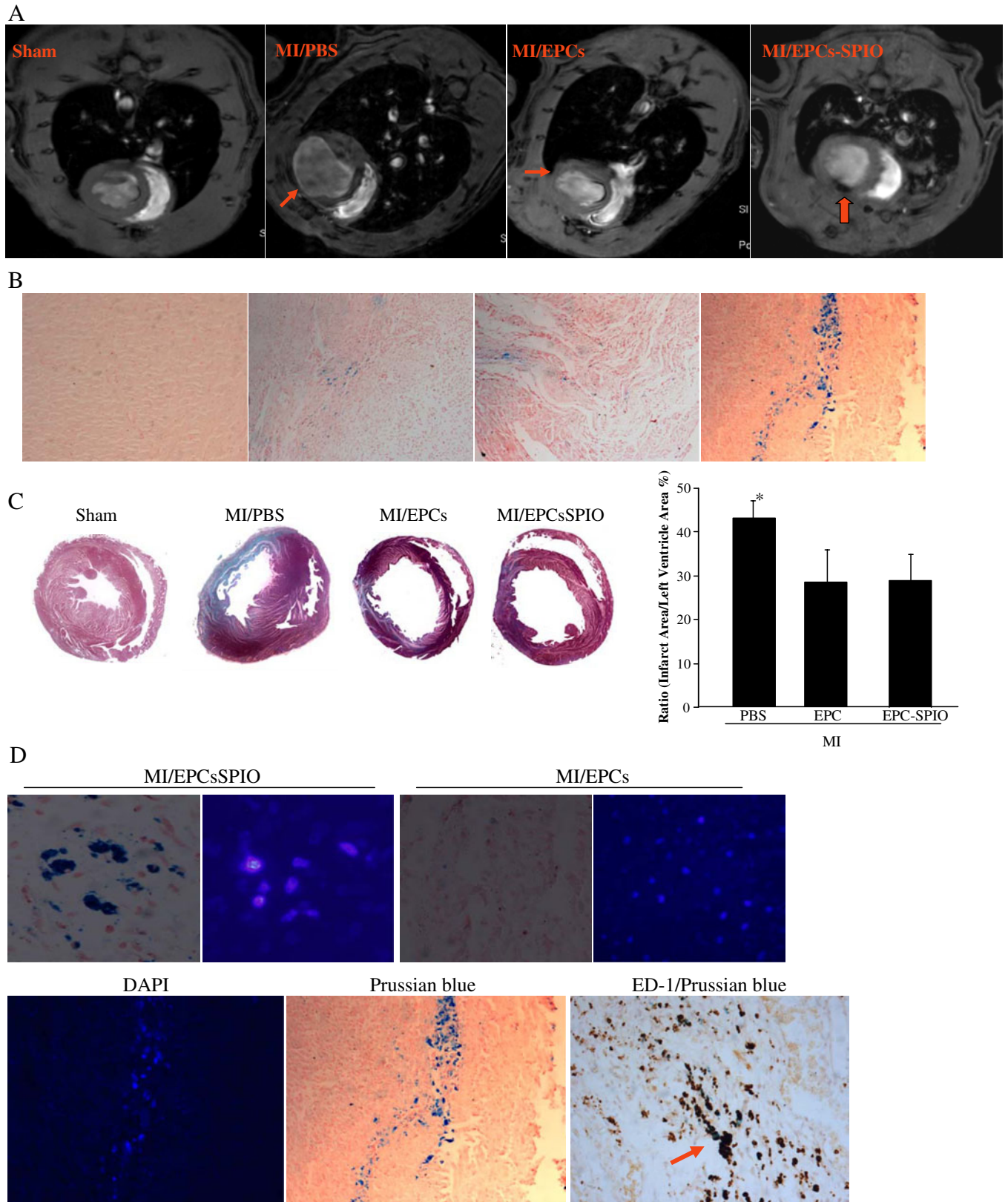
EPC transplantation significantly increased the expression level of VEGF in the infarct area (Fig. 5d). Immunostaining showed that the EPC and EPCs-SPIO groups showed strong and extensive VEGF expression, especially in the border zone (Fig. 5a). The upregulated level of VEGF was associated with a significant increase in the amount of both capillaries and arterioles at 10 days after MI, as identified by immunostaining with antibodies to CD-31 and  $\alpha$ -SMA, respectively (Fig. 5b, c).

Quantitative analysis indicated that the capillary density was significantly increased in the EPC groups compared to the MI control group (Fig. 5d). Similarly, increased arteriole number was observed in both the labeled and unlabeled EPCs (Fig. 5f). These results indicate that BMEPCs are capable of promoting neovascularization after MI and that SPIO labeling does not decrease this effect.

### *The Fate of SPIO-Labeled and Unlabeled EPCs after Transplantation in MI*

To monitor the distribution and the fate of transplanted cells, EPCs were double-labeled with SPIO and DAPI. Rats with grafted SPIO/DAPI co-labeled cells were examined by MRI at different times after EPC transplantation. MR images were matched with postmortem histological sections as much as possible.

Grafted SPIO-labeled cells were visualized as hypointense areas by MRI 1 day after MI. No MR signal attenuation was observed in rats injected with unlabeled EPCs (Fig. 2c). In postmortem specimens, both Prussian blue staining and fluorescence microscopy revealed EPCs to be located in the infarcted region (Fig. 2e).



Ten days and 8 weeks after MI, serial follow-up MRI revealed that grafted SPIO-labeled cells are visualized as void signal. Prussian blue-positive cells were also detected in the specimens obtained at 10 days and 8 weeks after EPC

injection. Prussian blue staining and fluorescence microscopy confirmed the presence of implanted EPCs labeled with SPIO/DAPI 10 days after MI (Fig. 3d). There were no differences in DAPI-positive EPC number between the

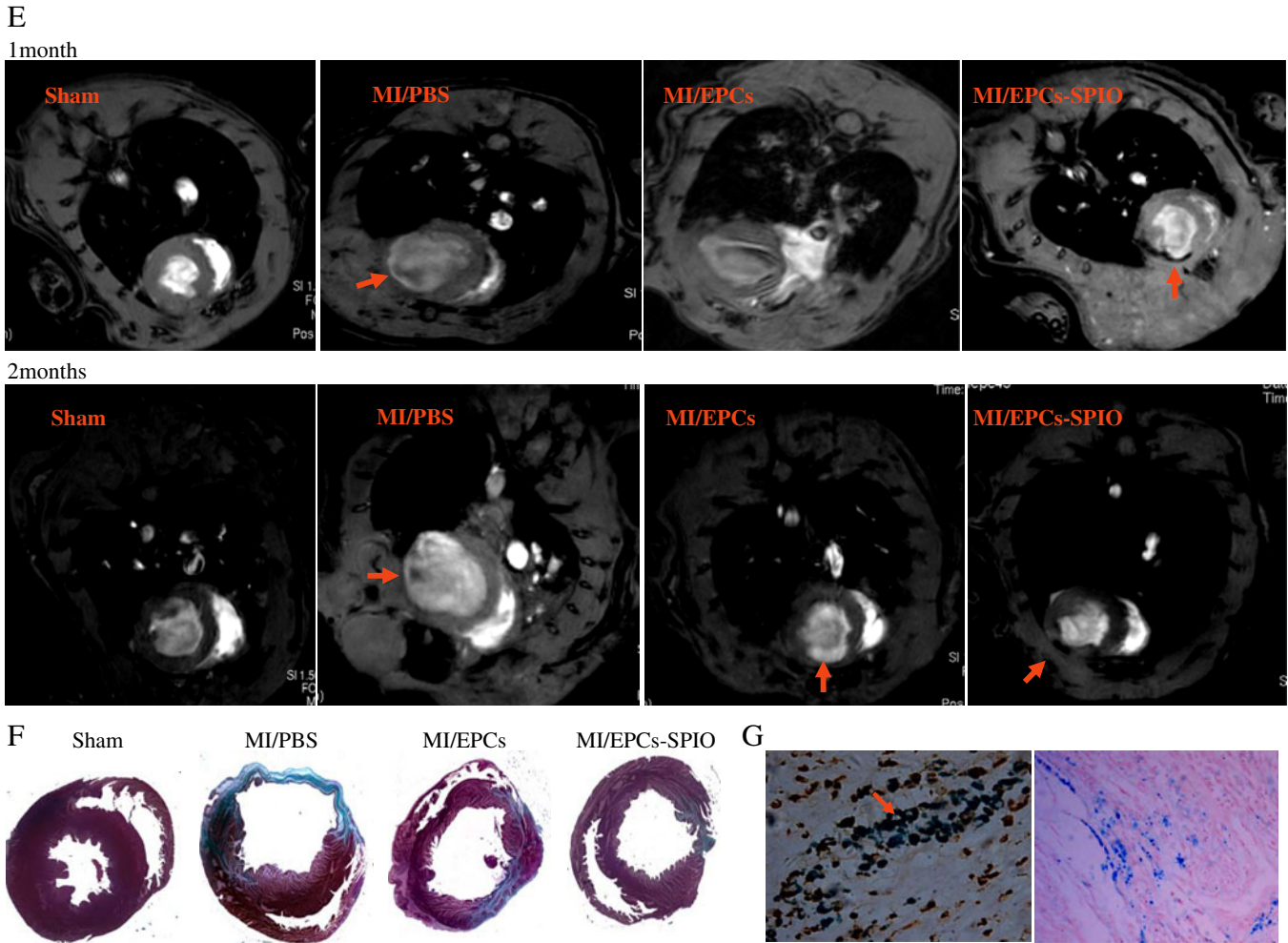


Fig. 3. (continued).

groups with and without SPIO labeling ( $11.8 \pm 2$  and  $11.8 \pm 3$ /field). Eight weeks after MI, no Prussian blue-positive cells were detected with DAPI-positive staining. However, those Prussian blue-positive cells were not represented as the originally grafted labeled cells. Prussian blue and macrophage marker ED-1 immunohistochemical double staining confirmed that Prussian blue-positive cells are macrophages

(Fig. 3g). Only several cells showed Prussian blue and ED-1 co-staining 10 days after MI (Fig. 3d).

### Discussion

The data presented in the current study demonstrate that the transplanted SPIO-labeled EPCs were not present in the

**Table 1.** Assessment of physiological parameters and the cardiac function by echocardiography in unlabeled cells, SPIO-labeled cells, and PBS-treated groups 10 days and 8 weeks after MI

Variable	Sham		MI		MI/EPCs		MI/EPCs-SPIO	
	10 days	8 weeks	10 days	8 weeks	10 days	8 weeks	10 days	8 weeks
HW/BW (mg/g)	$3.1 \pm 0.1$	$3.1 \pm 0.2$	$3.9 \pm 0.1$	$4.5 \pm 0.2$	$3.3 \pm 0.1^*$	$3.5 \pm 0.1^*$	$3.5 \pm 0.2^*$	$3.7 \pm 0.2^*$
EF (%)	$85.7 \pm 5.2$	$79.3 \pm 4.7$	$41.1 \pm 8.2$	$39.9 \pm 5.1$	$68.7 \pm 8^*$	$64.9 \pm 6.4^*$	$68.8 \pm 9.1^*$	$64.2 \pm 5.1^*$
FS (%)	$56.8 \pm 6.5$	$51.3 \pm 9.6$	$20.9 \pm 4.9$	$24.0 \pm 6.1$	$38.1 \pm 3.8^*$	$37.7 \pm 3.9^*$	$40.1 \pm 7.5^*$	$36.6 \pm 8.5^*$
LVIDd (mm)	$6.5 \pm 0.5$	$6.3 \pm 0.6$	$7.8 \pm 0.7$	$7.6 \pm 0.5$	$6.5 \pm 0.7^*$	$6.4 \pm 0.4^*$	$6.6 \pm 0.7^*$	$6.4 \pm 0.7^*$
LVIDs (mm)	$2.6 \pm 0.6$	$2.6 \pm 0.7$	$5.8 \pm 1.1$	$5.2 \pm 0.6$	$4.0 \pm 1.1^*$	$3.8 \pm 0.4^*$	$4.1 \pm 0.7^*$	$3.9 \pm 1.0^*$

Values are mean  $\pm$  SEM;  $n=5$  in each group

MI myocardial infarction, EF ejection fraction, LVIDd left ventricular inner diastolic diameter, LVIDs left ventricular inner systolic diameter

\* $P < 0.05$  (vs. MI and sham)



**Table 2.** Effects of EPC transplantation on cardiac function and hemodynamics 8 weeks after MI

Variable	Sham	MI	MI/EPCs	MI/EPCs-SPIO
MPA (mmHg)	91.5±19.7	55.6±10.4	87.9±14*	74.1±5.1*
LVEDP (mmHg)	5.9±2.1	29.8±12.5	11.4±2.3*	18.1±6.1*
dP/dt max (mmHg/s)	4,781.5±798	2,689±544	3,633.5±272*	3,724.3±172*
dP/dt min (mmHg/s)	4,627±1,036	2,264±408	3,201±276*	3,424±662*

Values are mean ± SEM; n=5 in each group

MI myocardial infarction

\*P<0.05 (vs. MI and sham)

infarcted myocardium at 8 weeks. Postmortem histological analysis showed that enhanced MRI signals arose from macrophages, although only a few grafted cells survived in the 10-day groups. Both labeled and unlabeled cells maintain their protective effect against progressive LV dilatation and dysfunction. The major mechanism appears to be paracrine pathways of the engrafted EPCs, resulting in the prevention of apoptosis and enhanced neovascularization of ischemic myocardium.

The development of molecular imaging techniques has enabled the noninvasive assessment of cell location, migration, and proliferation *in vivo* [13]. Labeling with iron particles and tracking cell fate by MRI provide a means of identifying and tracking the migration of labeled cells *in vivo* [14]. In the present study, commercially available agent

Resovist was successfully used to label cells, and our results showed that the Resovist/poly-L-lysine method was very efficient. *In vitro* MRI can efficiently detect low numbers of SPIO-labeled EPCs and that the intensity of the signal is proportional to the number of labeled cells.

A major advantage of the approach used here is that MRI affords the opportunity to simultaneously acquire data about cardiac structure and cell tracking capabilities. Using a 7.0-T scanner to identify transplanted cells, we were able to detect the intramyocardial injection sites of labeled EPCs in the rat heart by *in vivo* MRI. From 1 day to 8 weeks after MI, intracellular SPIO of transplanted cells could be readily detected as dark spots, though at 8 weeks, the signal size decreased. Successful cell engraftment was evidenced by

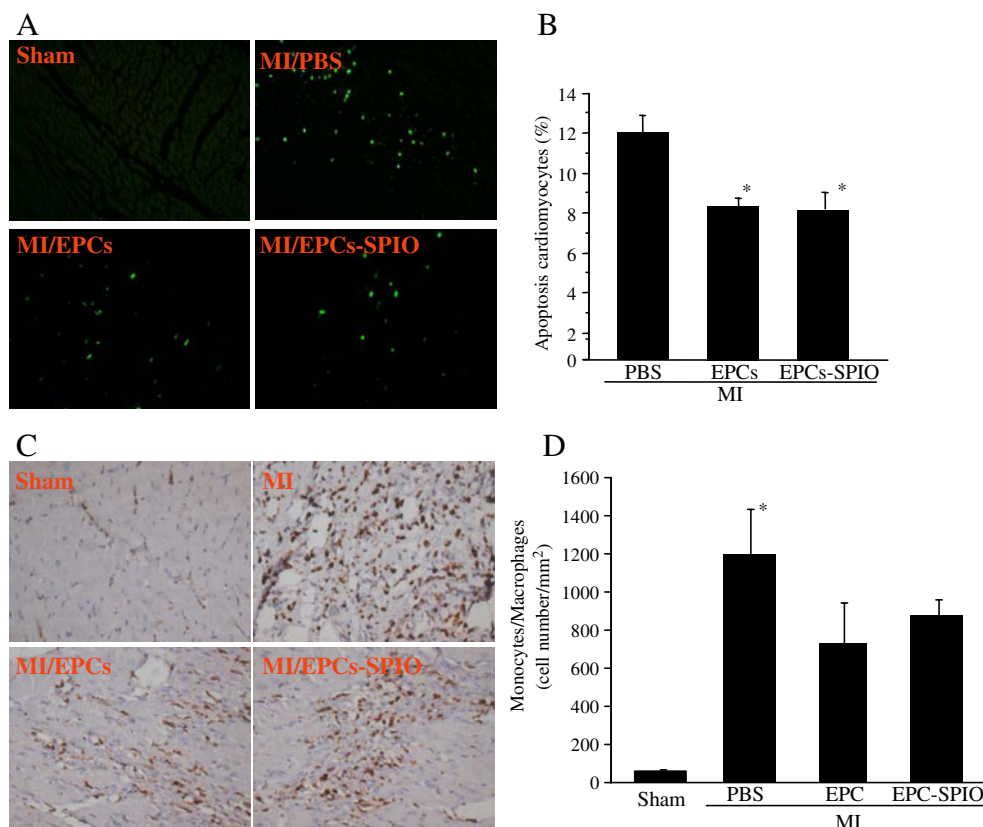


**Fig. 4.** EPC transplantation treatment reduces cardiomyocyte apoptosis and monocyte/macrophage accumulation 10 days after MI. **a** Representative micrographs show TUNEL-positive apoptotic cardiomyocytes from the peri-infarcted zone of rat hearts (×200 magnification). **b** Quantitative analysis of apoptotic cardiomyocytes expressed as percentage of TUNEL-positive nuclei in cardiomyocytes. TUNEL-positive non-cardiomyocytes were excluded. **c** Representative images of ED-1 immunostaining in the infarcted area (×200 magnification). **d** Quantitative analysis of ED-1-positive cells.

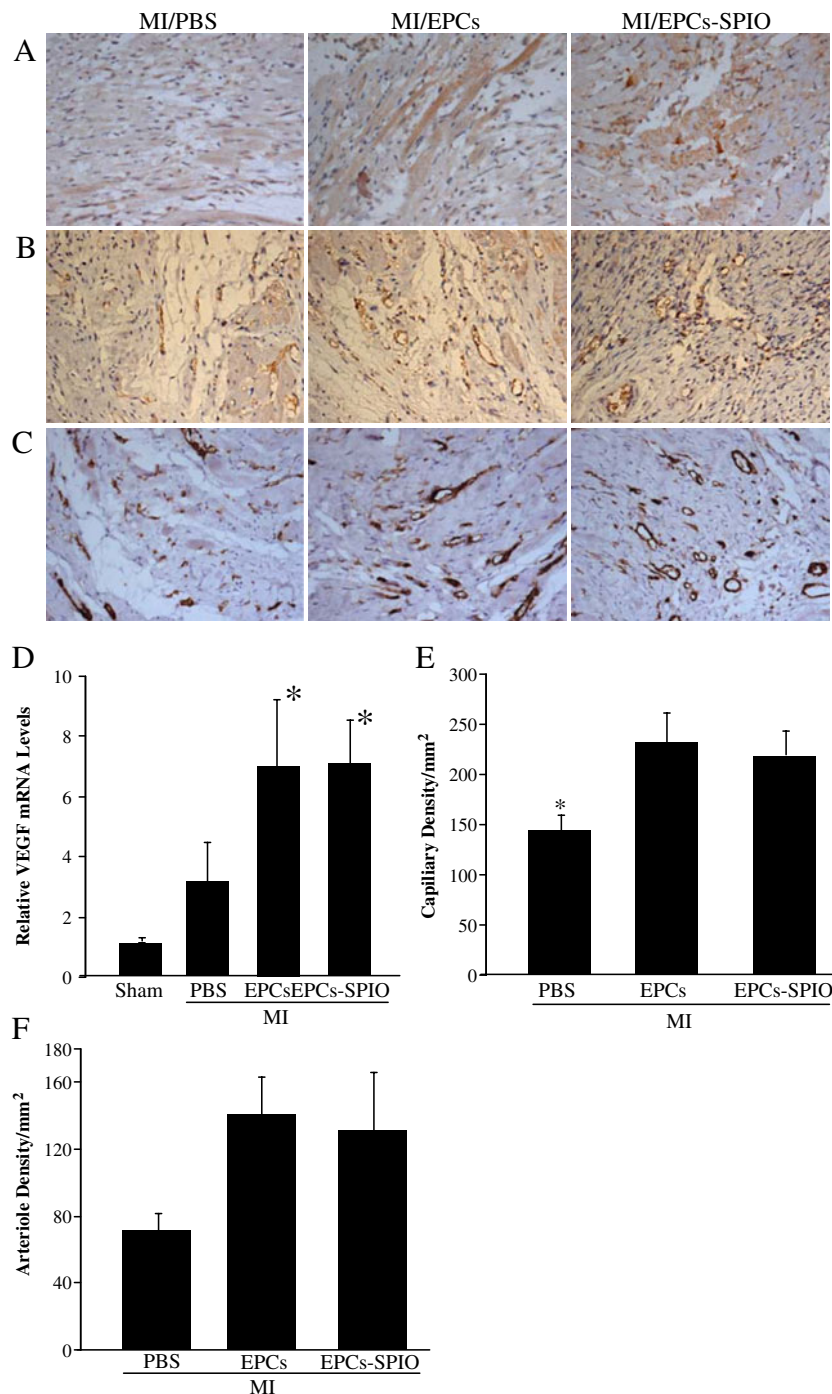


**Fig. 5.** EPC transplantation promotes neovascularization 10 days after MI. Representative micrographs of heart sections stained with antibodies against VEGF (a), CD31 (b), and  $\alpha$ -SMA (c) ( $\times 200$  magnification). d VEGF mRNA levels determined by real-time PCR. Values are expressed as mean  $\pm$  SEM ( $n=6$ ,  $*P<0.05$  vs. MI). e Capillary density expressed as capillaries per square millimeter. f Arteriole density in the peri-infarct area, expressed as the number of vessels per field.

numerous DAPI and Prussian blue double-stained cells at the site of injection 24 h after injection. But at 8 weeks after MI, according to DAPI fluorescence, neither labeled nor unlabeled cells survived in the infarcted myocardium. In addition, numerous Prussian blue-stained cells were positive for ED-1 immunostaining, indicating that Prussian blue-positive cells represent phagocytic macrophages that contain

native iron or had ingested Resovist from lysed EPCs. But in the 10-day groups, a few Prussian blue and DAPI double-positive cells were observed and were negative for ED-1 immunostaining; only several cells were positive for iron and ED-1 co-staining. Amsalem et al. [15] has reported that at 4 weeks after transplantation of SPIO-labeled MSCs, the transplanted cells are not present in the scar and that the

enhanced MRI signals arise from cardiac macrophages that engulf the SPIO. Some studies showed that MRI overestimated iron-labeled stem cell survival after transplantation in the heart [16, 17]. However, Sadek and Garry [18] believed that the conclusion was misleading, inferring that Amsalem and coworkers delivered immunogenic cells (MSCs) into an immunocompetent model in the absence of immunosuppressive agents, resulting in the complete elimination of the iron oxide nanoparticle-labeled MSCs from the recipient heart. Thus, we used cyclosporin A as an immunosuppressive agent, but got similar results compared to Amsalem. We presume that cellular rejection is not the main cause of macrophage appearance. In acute MI, myocardial tissue damage causes cell death and macrophage infiltration, leading to the engulfment of dying and discarded host cells by macrophages. Taken together, our data indicate that SPIO labeling is a better marker for a high-resolution detection of cell location by MR in the early stage of repair from MI. A fundamental drawback of MRI for cell tracking is the difficulty in distinguishing iron-labeled cells from the free iron released upon cell death.

As shown in Tables 1 and 2, we used two methods to evaluate cardiac function at 10 days and 8 weeks after MI. The results consistently show that both labeled and unlabeled EPCs attenuated LV dysfunction. Cardiac MRI can provide non-invasive, high-resolution images of heart anatomy, viability, perfusion, and function. However, in this study, functional evaluation using high-field MRI was not undertaken because we do not have the appropriate software to analyze the results.

EPCs possess a potential for augmented neovascularization and functional preservation of the left ventricle in acute myocardial ischemia [19]. We showed that VEGF levels are upregulated by both labeled and unlabeled EPCs and are associated with a significantly increased number of capillaries and arterioles in the peri-infarct area. In addition to their role as a structural tissue component, EPCs express many factors that contribute to tissue regeneration and preservation, including pro-angiogenic and anti-apoptotic growth factors (e.g., VEGF, hepatocyte growth factor, etc.) [18]. Our results showed that labeled and unlabeled EPCs enhanced cardiac function after MI, although relatively few cells survived in the ischemic tissue and no DAPI-positive cell incorporation into vascular structures was observed. The disproportionately large improvement in functional outcome in rats treated with EPCs compared to the actual number of EPCs present in the ischemic tissue indicates that the restorative effect of EPCs is not due to transdifferentiation of the transplanted cells. We found a markedly decreased ratio of cardiomyocyte apoptosis and macrophage infiltration 10 days after MI, which is most likely a paracrine effect of EPCs.

To the best of our knowledge, to further evaluate the duration of transplanted cell survival, integration, and proliferation in target organs, multimodality imaging techniques combined with the relative advantages of MRI, PET, SPECT, optical imaging, and ultrasound will provide complementary and reliable information to assess stem cell engraftment in the recipient tissue.

*Acknowledgments.* We would like to thank Drs. Fang Fang and Fengchao Zang for their help with rodent imaging. Finally, we would like to acknowledge the grant support for our laboratory from the National Natural Science Foundation of China (30871071).

*Conflict of interest.* The authors declare no conflict of interest.

## References

1. Kiernan TJ, Yan BP, Jaff MR (2009) Antiplatelet therapy for the primary and secondary prevention of cerebrovascular events in patients with extracranial carotid artery disease. *J Vasc Surg* 50:431–439
2. Schachinger V, Erbs S, Elsasser A et al (2006) REPAIR-AMI investigators intracoronary bone marrow-derived progenitor cells in acute myocardial infarction. *N Engl J Med* 355:1210–1221
3. Beines JO, Hopp E, Lunde K et al (2009) Long-term results after intracoronary injection of autologous mononuclear bone marrow cells in acute myocardial infarction: the ASTAMI randomised, controlled study. *Heart* 95:1983–1989
4. Lunde K, Solheim S, Aakhus S et al (2006) Intracoronary injection of mononuclear bone marrow cells in acute myocardial infarction. *N Engl J Med* 355:1199–1209
5. Reinlib L, Field L (2000) Cell transplantation as future therapy for cardiovascular disease? A workshop of the National Heart, Lung, and Blood Institute. *Circulation* 101:E182–E187
6. Espinosa-Heidmann DG, Reinoso MA et al (2005) Quantitative enumeration of vascular smooth muscle cells and endothelial cells derived from bone marrow precursors in experimental choroidal neovascularization. *Exp Eye Res* 80:369–378
7. Heyn C, Ronald JA, Ramadan SS et al (2006) *In vivo* MRI of cancer cell fate at the single-cell level in a mouse model of breast cancer metastasis to the brain. *Magn Reson Med* 56:1001–1010
8. Yeh TC, Zhang W, Ildstad ST, Ho C (1993) Intracellular labeling of T-cells with superparamagnetic contrast agents. *Magn Reson Med* 30:617–625
9. Himes N, Min JY, Lee R et al (2004) *In vivo* MRI of embryonic stem cells in a mouse model of myocardial infarction. *Magn Reson Med* 52:1214–1219
10. van den Bos EJ, Wagner A, Mahrholdt H et al (2003) Improved efficacy of stem cell labeling for magnetic resonance imaging studies by the use of cationic liposomes. *Cell Transplant* 12:743–756
11. Dick AJ, Guttman MA, Raman VK et al (2003) Magnetic resonance fluoroscopy allows targeted delivery of mesenchymal stem cells to infarct borders in swine. *Circulation* 108:2899–2904
12. Rafii S, Lyden D (2003) Therapeutic stem and progenitor cell transplantation for organ vascularization and regeneration. *Nat Med* 9:702–712
13. Swijnenburg RJ, van der Bogt KEA, Sheikh et al (2007) Clinical hurdles for the transplantation of cardiomyocytes derived from human embryonic stem cells: role of molecular imaging. *Curr Opin Biotechnol* 18:38–45
14. Hoehn M, Küstermann E, Blunk J et al (2002) Monitoring of implanted stem cell migration *in vivo*: a highly resolved *in vivo* magnetic resonance imaging investigation of experimental stroke in rat. *Proc Natl Acad Sci USA* 99:16267–16272
15. Amsalem Y, Mardor Y, Feinberg MS et al (2007) Iron-oxide labeling and outcome of transplanted mesenchymal stem cells in the infarcted myocardium. *Circulation* 116(11 Suppl):I38–I45
16. Li Z, Suzuki Y, Huang M et al (2008) Comparison of reporter gene and iron particle labeling for tracking fate of human embryonic stem cells and differentiated endothelial cells in living subjects. *Stem Cells* 26:864–873
17. Terrovitis J, Stuber M, Youssef A et al (2008) Magnetic resonance imaging overestimates ferumoxide-labeled stem cell survival after transplantation in the heart. *Circulation* 117:1555–1562
18. Sadek HA, Garry DJ (2008) Letter by Sadek and Garry regarding article, “Iron-oxide labeling and outcome of transplanted mesenchymal stem cells in the infarcted myocardium”. *Circulation* 117:e306
19. Urbich C, Aicher A, Heeschen C et al (2005) Soluble factors released by endothelial progenitor cells promote migration of endothelial cells and cardiac resident progenitor cells. *J Mol Cell Cardiol* 39:733–742